Petroleum Science 18 (2021) 1689–1697

Contents lists available at ScienceDirect

Petroleum Science

journal homepage: www.keaipublishing.com/en/journals/petroleum-science

Original Paper

Mechanical behavior of drillstring with drag reduction oscillators and its effects on sliding drilling limits

Xiao-Lei Shi, Wen-Jun Huang*, De-Li Gao**

MOE Key Laboratory of Petroleum Engineering, China University of Petroleum, Beijing, 102249, China

ARTICLE INFO

Article history:
Received 23 November 2020
Accepted 24 May 2021
Available online 2 September 2021

Edited by Yan-Hua Sun.

Keywords:
Drillstring
Downhole oscillator
Friction force
Drag reduction
Sliding drilling

ABSTRACT

Practice has proved that drag reduction oscillators can decrease the axial friction and increase wellbore extension effectively in sliding drilling operations. However, the complicated mechanical behavior of drillstring with drag reduction oscillators has not been revealed sufficiently. In this paper, the mechanical model of drillstring with drag reduction oscillators is established by considering the friction nonlinearity. Further introducing the initial conditions, boundary conditions and continuity conditions, the finite differential equation of drillstring vibration is obtained and solved. The new model has been applied to a case study, in which the drag reduction effects of drillstring with and without oscillators are compared and the effects of relevant factors on drag reduction are analyzed. The results show that the hook loads increase obviously by reducing downhole average friction coefficient for drillstring with oscillators. Increasing vibration amplitude of the drag reduction oscillator can decrease axial friction, but the vibration frequency is nearly irrelevant to drag reduction. Increasing number of drag reduction oscillators can decrease axial friction, but may lead to large hydraulic power loss and high risk of drillstring fatigue. Therefore, there is an optimal number of drag reduction oscillators. The research results are of significant guiding significance for optimal design and safety control in sliding drilling operations.

1. Introduction

In recent years, with the rapid development of drilling technology, well depth has been continuously extended. Complex structure wells such as horizontal wells and extended reach wells have been more widely used in oil & gas exploration and development. Compared with conventional well types, complex structure wells are facing many technical problems. Especially in the long horizontal section drilling process, large friction and pipe sticking occurs frequently, causing low efficiency of normal drilling or even serious drilling accident. To effectively reduce the friction between drillstring and borehole wall, not only the average friction force should be reduced, but also the static friction force should be changed into dynamic friction force. Practice has proved that drag reduction oscillator can decrease the friction force and increase the wellbore extension a lot. At present, the vibration drag reduction tools abroad are mainly divided into two types: mechanical vibration and hydraulic vibration. Mechanical vibration is represented by Agitator hydraulic oscillator, and hydraulic vibration is represented by friction drag reducer (FDR) tool. The agitator hydraulic oscillator (Newman et al., 2009; Skyles et al., 2012) can generate an impact force of 3.45–4.14 MPa due to changes in frequency, amplitude, outer diameter and length. Through axial vibration, the sliding friction can be reduced by 75%–80%. The required weight on bit with the tools is about 60% of that without the tools, and all measurements while drilling (MWD) will not be disturbed by Agitator tools. Meanwhile, the axial vibration generated by Agitator tool will not damage the bearings and teeth of drill bit. Agitator hydraulic oscillator has been applied in many oil fields around the world and achieved good results. It can greatly reduce the friction in sliding drilling and improve the penetration rate a lot. The FDR tool (Sola et al., 2000) was developed by RF-Rogaland Research. The tool is mainly composed of a two-way moving hydraulic cylinder with an inner valve and an outer valve. It has been comprehensively tested in actual drilling processes and the results show that the friction on coiled tubing can be reduced by 90%. In order to improve axial force transmission in extended reach wells, Sinopec has

* Corresponding author.
** Corresponding author.
E-mail addresses: huangwenjun1986@126.com (W.-J. Huang), gaodeli@cup.edu.cn (D.-L. Gao).

https://doi.org/10.1016/j.petsci.2021.09.007

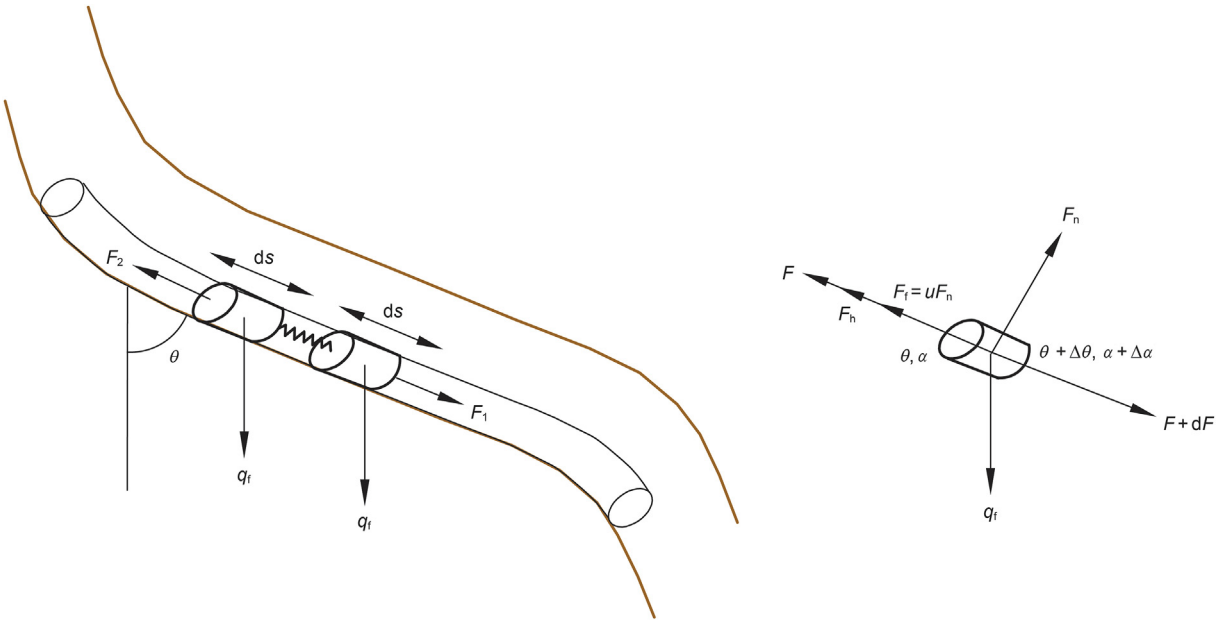

Fig. 1. Stress state of differential element of drillstring while drilling.

developed a SLZDDQ172 hydraulic pulse oscillation tools (Zhang et al., 2014). The tool has an outer diameter of 172 mm, a working frequency of 15 Hz, a working pressure loss of 3–4 MPa, and a displacement of 10–30 L/s. It can increase the penetration rate by more than 20%. CNPC Daqing Drilling Engineering Company has designed a set of hydraulic oscillators (Li, 2014). The vibration frequency is 16 Hz, the amplitude is 4 mm, the pressure drop is 2 MPa at wellhead, and the reliability of the tool is verified through indoor and field tests. The research and development of the new turbine hydraulic oscillator (Wang et al., 2016) has been in testing stage in the laboratory, and field application has not been carried out. Other vibration drag reduction tools are developed and improved based on the principle of Agitator tools.

The studies of tubular mechanics has been for more than 70 years and a lot of innovative research results have been obtained. Baker et al. (1952) found that when a small mechanical vibration occurs, the friction in the contact systems will be greatly reduced. Fridman et al. (1959) concluded that friction resistance between the contact surfaces under ultrasonic vibration will be significantly reduced through experiment. Pohlman et al. (1966) found that vibration can reduce the friction between the contact surfaces through large scale motion analysis. Johancsik et al. (1984) established a soft rope model using model analysis method and predicted the pulling force of drillstring, which provides theoretical basis for wellbore trajectory design and drillstring optimization. Ho (1988) established a new stiffness model that considered the three factors of drillstring rigidity on the basis of Johancsik et al. (1984)'s model. Lin et al. (1990) verified Denison's theory (Denison, 1979) and proposed that beating in drilling is induced by the nonlinearity of the total resistance to the drilling (dry friction, viscous damping and torque on bit). The formation of three-lobe pattern at the hole bottom and self-excited vibration without the bit being stuck are also explored. Li et al. (2004) established a mathematical model of drillstring longitudinal vibration analysis with bit displacement and bit stress as boundary conditions and a mathematical model of drillstring torsional vibration analysis with bit rotation and bit torque as boundary conditions, respectively. It is concluded that the longitudinal vibration of drillstring should be studied with bit displacement as the boundary condition and the torsional vibration

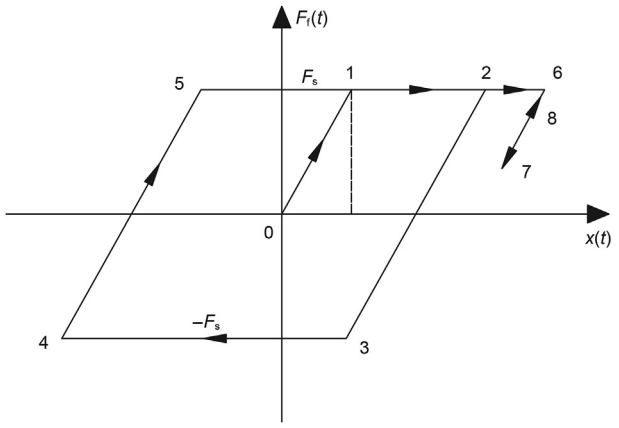

Fig. 2. Typical double-fold constitutive relation.

of drillstring should be studied with bit rotation as the boundary condition. Baez et al. (2011) investigated the application of hydraulic oscillators in the United States, and found that hydraulic oscillators can reduce the friction force on the drillstring and improve weight on bit. Field application in hundreds of wells indicates that hydraulic oscillators can increase the penetration rate by 37% and greatly improve the construction efficiency. Liao et al. (2012) studied drillstring motions by experimental and numerical investigations. The numerical efforts are carried out by using a reduced-order model with attention to stick-slip interactions between a drill string and an outer shell. These efforts are complemented by experimental studies conducted with a unique, laboratory scale model. By analyzing the principle of sliding drilling, Li et al. (2013) found that the application of hydraulic oscillator can reduce the sliding friction and increase the length of single drilling during sliding drilling. Liu et al. (2014) developed a two degree-of-freedom model considering state-dependent time delay and nonlinearity to study the coupled axial-torsional dynamics. Next, Liu et al. (2020) developed and studied an integrated model with spatially distributed inertia and general boundary conditions

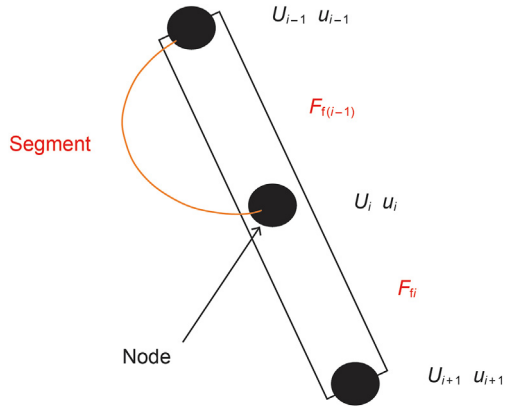

Fig. 3. Schematic diagram of discretization parameters of drillstring.

for the axial-torsional dynamics of a drill string again. Miska et al. (2015) established an improved soft rod dynamic model based on the movement of drill pipe in 2D and 3D boreholes. Bavadiya et al. (2017) conducted on a fully automated drilling rig to examine the effects of drilling parameters on drillstring vibrations, torque and rate of penetration. AlZibde et al. (2017) studied a novel approach to mitigate undesired vibrations, the effects of adding a sinusoidal input to the rotation speed of a drill string. Wang et al. (2018) considered the transformation and decomposition mechanism of static friction force and dynamic friction force, and established a friction reduction model which was solved by second-order finite difference method and analyzed the vibration behavior and parameters under different axial load transfer and tool surfaces. Zheng et al. (2020) considered nonlinear effects associating with dry friction, loss of contact and the state-dependent delay, and studied a reduced-order drillstring model with coupled axial and torsion dynamics.

It can be found that previous studies are mainly focused on design and application of drag reduction tools, but the theoretical studies on drag reduction tools are rare. Moreover, the nonlinearity of friction force has not been sufficiently considered in the conventional models. In this paper, the mechanical model of drillstring with drag reduction oscillator is built while considering friction nonlinearity, and the model is solved with finite differential method. The new model is applied to a case study to reveal the effects of relevant parameters on drag reduction.

2. Theoretical model

The following assumptions are made:

(1) The drillstring is an elastic rod, the cross-sectional area is circular, and the inner wall of the borehole is rigid.
(2) The drillstring is in uniform contact with the borehole wall without rotation.
(3) Axial vibration is considered, but lateral and torsional vibrations are neglected.
(4) The bilinear hysteretic restoring force model is adopted to depict the friction between the drillstring and the wellbore.
(5) The vibration drag reduction oscillator is simplified as a spring with greater rigidity.

2.1. Differential equation

As shown in Fig. 1, the drillstring is composed of multiple differential element segments, and the force analysis of one differential element is performed. Assuming that the entire drillstring is in static state under initial condition. Thus, the equilibrium equation of the differential element of drillstring can be written as:

$$F + \mathrm{d}F + q_e\cos\theta \mathrm{d}s - F - \pi D_o C v \mathrm{d}s - \mu\rho_s A_s g\sin\theta \mathrm{d}s = 0 \tag{1}$$

Since $F = EA_s\frac{\partial U}{\partial s}$, the above equation can be re-written as:

$$\frac{\partial^2 U}{\partial s^2} = \frac{\mu\rho_s A_s g\sin\theta + \pi D_o C v - q_e\cos\theta}{EA_s} \tag{2}$$

$$q_e = \rho_s A_s + \rho_i A_i - \rho_o A_o \tag{3}$$

During the vibration process, the oscillator can apply regular excitation force to the drillstring. The static friction force between the drillstring and the borehole wall is converted into dynamic friction force. Under the action of the weight, friction force, weight on bit and viscous force, the vibration equation of the drillstring is written as follows:

$$F + \mathrm{d}F + q_e\cos\theta \mathrm{d}s - F - \pi D_o C\left(\frac{\partial U}{\partial t} + v\right)\mathrm{d}s - F_f \mathrm{d}s = \rho_s A_s \mathrm{d}s\frac{\partial^2 U}{\partial t^2} \tag{4}$$

The above equation can be re-written as:

$$\frac{E}{\rho_s}\frac{\partial^2 U}{\partial s^2} + \frac{q_e\cos\theta}{\rho_s A_s} - \frac{\pi D_o C}{\rho_s A_s}\left(\frac{\partial U}{\partial t} + v\right) - \frac{F_f}{\rho_s A_s} = \frac{\partial^2 U}{\partial t^2} \tag{5}$$

$$C = \frac{2\zeta\lambda}{D_o \ln\frac{D_w}{D_o}} \tag{6}$$

where U is the axial displacement function; E is elastic modulus; μ is friction coefficient; ρ_s, ρ_i, ρ_o are the densities of drillstring, inner fluid and annular fluid; D_o, D_w are the outer diameter of drillstring and hole diameter; A_s, A_i, A_o are the cross-sectional area, inner area and outer area of drillstring, respectively; q_e is the equivalent drillstring weight per unit length; F_f is the friction force between the drillstring and the borehole wall (casing); v is the difference between the fluid velocity and the drillstring velocity; s is the distance from any point of the drillstring to the top of the section; C is a constant; ζ is the dynamic viscosity of the drilling fluid; λ is the coefficient of resistance increase caused by drillstring eccentricity; t is time; g is gravitational acceleration; θ is the angle of inclination.

2.2. Friction model

Iwan et al. (1961) put forward a bilinear hysteretic restoring force model, which equates the dry friction surface with a spring and an ideal Coulomb friction pair connected in series. the nonlinear restoring force F_f with memory characteristics is approximately described by a double fold line model. In this paper, the bilinear hysteretic restoring force model is adopted to depict the friction between the drillstring and the wellbore. As shown in Fig. 2 below, the constitutive relation in incremental form can be written as follows:

$$\begin{cases} \mathrm{d}F_f = \dfrac{k_s}{2}\left[1 + \mathrm{sgn}\left(F_s - \left|F_f\right|\right)\right]\mathrm{d}x \\ k_s = \dfrac{F_s}{x_s} \end{cases} \tag{7}$$

where x_s is the limit value of elastic deformation when the contact surface of the dihedral slides macroscopically; F_s is the memory

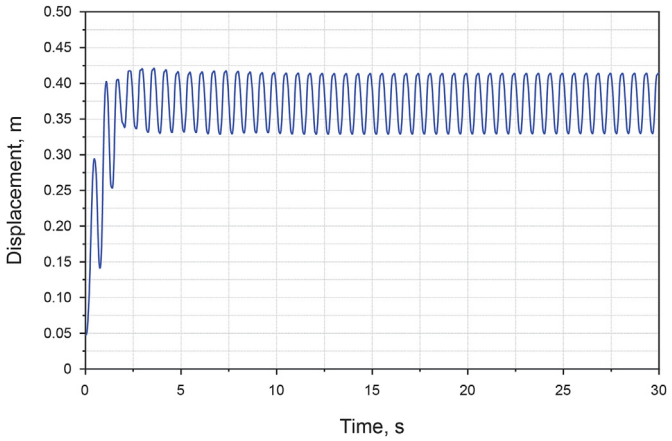

Fig. 4. Displacement change of drillstring at 600 m hole depth in sliding drilling operations.

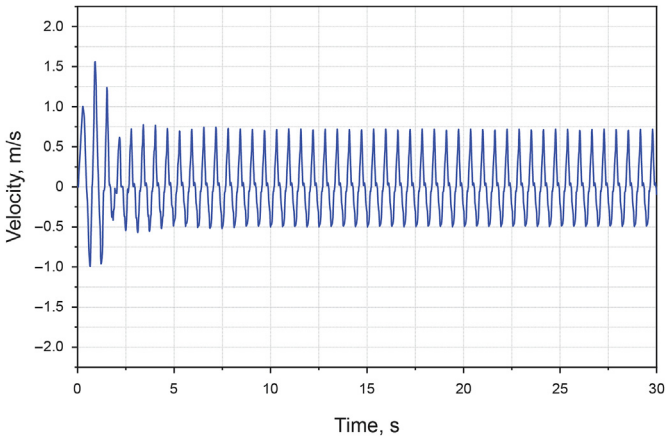

Fig. 6. Velocity change of drillstring at 600 m hole depth in sliding drilling operations.

restoring force when slipping; x is the relative displacement deformation of the two ends of the hysteresis link; k_s is the linear stiffness before the dry friction link slips.

3. Calculation method

3.1. Finite difference method

Fig. 3 is a schematic diagram of discretization of drillstring. Each drillstring is discretized according to the spatial step size, and a segment of drillstring has two nodes. The axial displacement U_i is defined on the nodes, and the F_{fi} is defined on the drillstring segment. The subscript "i" in displacement U_i represents the node to the left node of i-th segment or the right of node of $(i-1)$-th segment, and the subscript "i" in F_{fi} represents i-th segment.

In order to describe the variation between sliding friction and viscous friction, it is necessary to introduce a small time step in the finite difference calculation process. Explicit difference scheme is superior for calculation, because it is much faster than implicit method.

With the definitions of above discretized parameters, the explicit central difference scheme of Eq. (2) and Eq. (5) can be expressed as:

$$\frac{U_{i+1}^j - 2U_i^j + U_{i-1}^j}{\Delta s_i^2} = \frac{\mu_i^j \rho_s A_s g \sin\theta + \pi D_o C v_i^j - q_e \cos\theta}{EA_s} \tag{8}$$

$$\frac{E}{\rho_s}\frac{U_{i+1}^j - 2U_i^j + U_{i-1}^j}{\Delta s_i^2} + \frac{q_e \cos\theta}{\rho_s A_s} - \frac{\pi D_o C}{\rho_s A_s}\left(\frac{U_i^{j+1} - U_i^j}{\Delta t} + v_i^j\right) - \frac{F_{fi}}{\rho_s A_s} = \frac{U_i^{j+1} - 2U_i^j + U_i^{j-1}}{\Delta t^2} \tag{9}$$

where Δt is the time interval, the superscript "j" in U_i^j represents the j-th time point.

3.2. Initial condition

In general, the calculation of vibration equations requires initial conditions. The discretization scheme of the initial displacement can be expressed as:

$$U_i^1 = u_{\text{initial}} \tag{10}$$

The values of u_{initial} are obtained by solving Eq. (8).

The discretized scheme of initial velocity condition is expressed as:

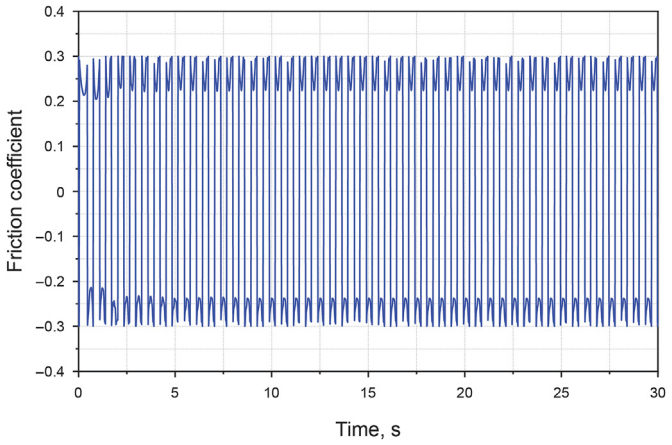

Fig. 5. Friction coefficient change of drillstring at 600 m hole depth in sliding drilling operations.

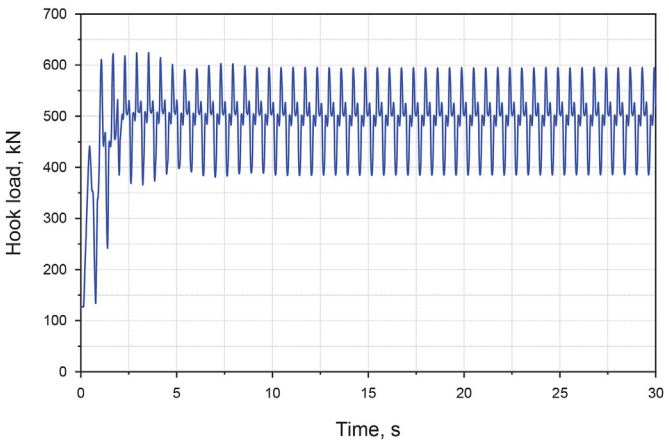

Fig. 7. Change of hook load in sliding drilling operations.

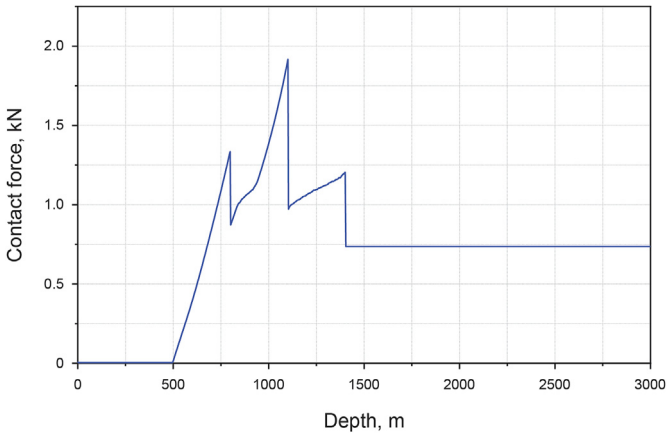

Fig. 8. Change of drillstring contact force during sliding drilling operations of 8 s time.

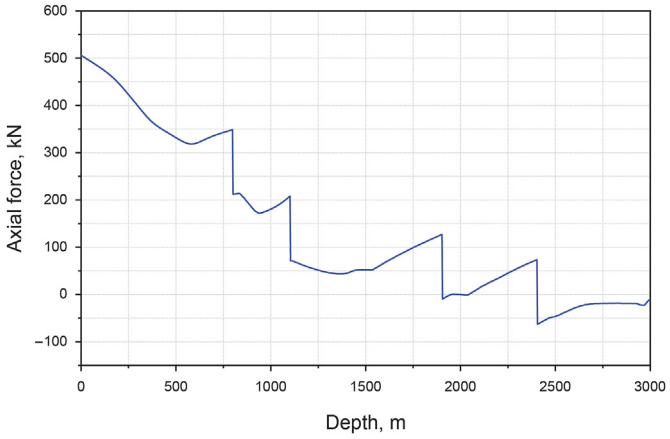

Fig. 9. Change of drillstring axial force during sliding drilling operation of 8 s time.

$$\frac{U_i^2 - U_i^0}{2\Delta t} = v_{\text{initial}} \tag{11}$$

Note that, the term U_i^0 in Eq. (11) can be eliminated by combing Eq. (9) and Eq. (11) while $j = 1$.

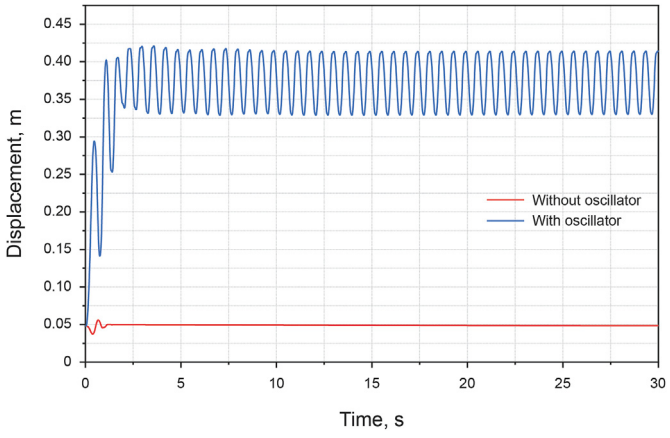

Fig. 10. Change of drillstring displacement in sliding drilling operations.

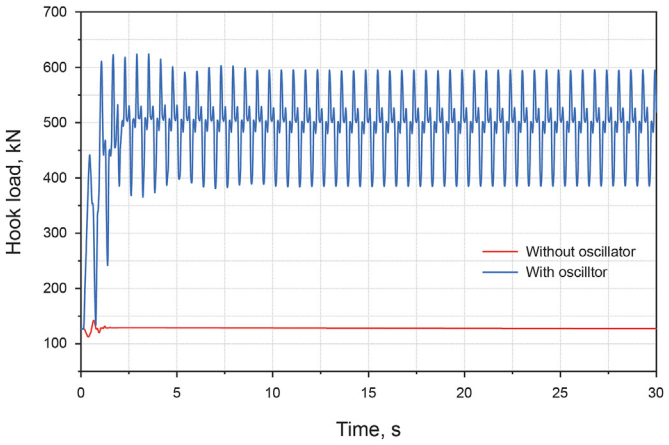

Fig. 11. Change of hook load in sliding drilling operation.

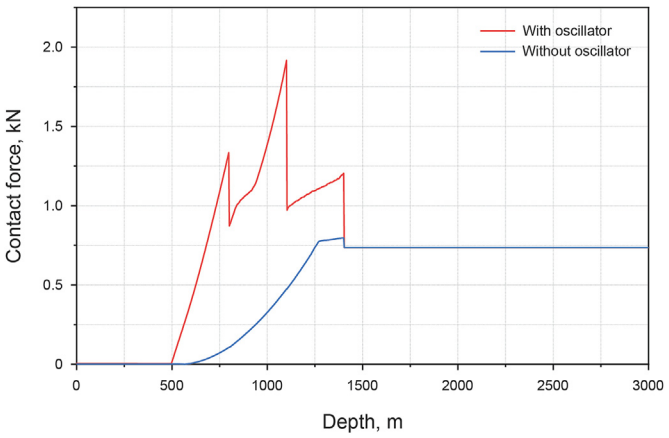

Fig. 12. Change of drillstring contract force in sliding drilling operations.

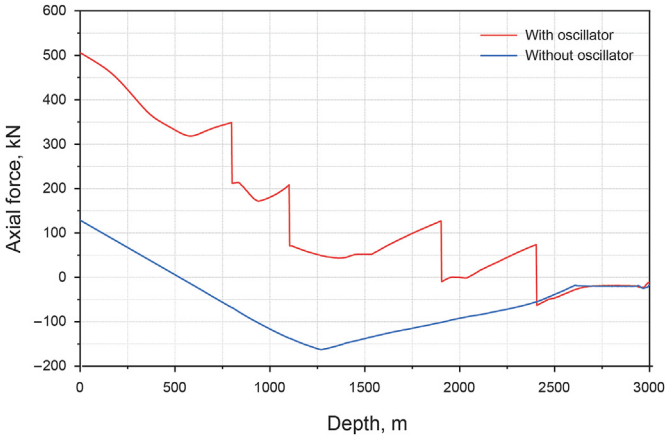

Fig. 13. Change of drillstring axial force in sliding drilling operations.

3.3. Boundary condition

The top of the drillstring is tied to hook, so the axial displacement of the top of drillstring is equal to the vertical displacement of the hook. Then, the top boundary condition is expressed as:

$$U_1^j = u_{\text{hook}} \tag{12}$$

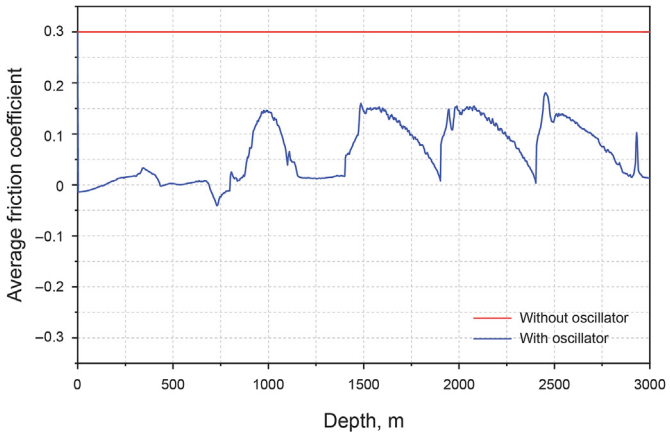

Fig. 14. Change of average friction coefficient of drillstring in sliding drilling operations.

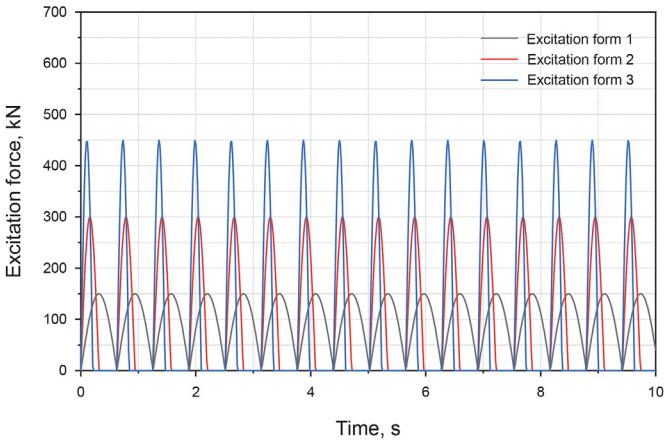

Fig. 15. The action form of the oscillator with excitation force.

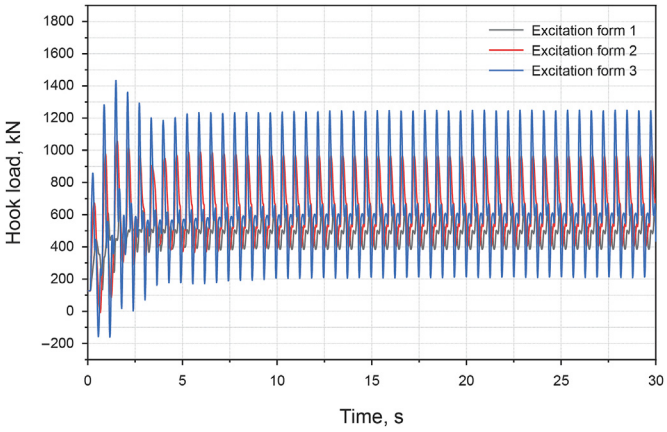

Fig. 16. Effect of the excitation force form on hook load.

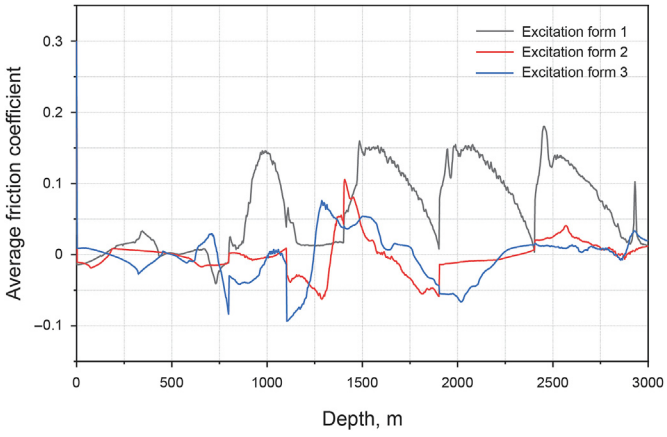

Fig. 17. Effect of the excitation force form on the average friction coefficient.

For the drillstring installed with an oscillator, an additional excitation force will be applied to the drillstring. Therefore, the boundary conditions at the upper and lower ends of the oscillator can be expressed as the axial force as:

$$(EA_s)_{i-1}\frac{U_i^j - U_{i-2}^j}{2\Delta s_{i-1}} = F_t + FF(t), (EA_s)_i\frac{U_{i+1}^j - U_{i-1}^j}{2\Delta s_i} = F_t \tag{13}$$

where F_t is the axial force at the joint of oscillator and drillstring; $FF(t)$ is the excitation force applied by the oscillator with time.

In the sliding drilling process, the axial force on bit is determined with bit-rock interaction model. Here, the axial force at the bottom of the drillstring is equal to the weight-on-bit value, namely

$$(EA_s)_n\frac{U_{n+1}^j - U_{n-1}^j}{2\Delta s_n} = Wob(t) \tag{14}$$

where $Wob(t)$ is the weight-on-bit which changes with time. Note that, the term U_{n+1}^j in Eq. (14) can be eliminated by combing Eq. (9) and Eq. (14) while $i = n$.

3.4. Continuous condition

When two or more than two kinds of drillstrings are adopted, the relevant parameters such as drillstring diameter, weight, etc. are discrepant for different drillstrings. Then the continuous conditions on the node connecting to different drillstrings should be satisfied. To be specific, the axial displacement and equivalent axial forces on adjacent segments are continuous, namely

$$(EA_s)_{i-1}\frac{U_i^j - U_{i-1}^j}{\Delta s_{i-1}} = (EA_s)_i\frac{U_{i+1}^j - U_i^j}{\Delta s_i} \tag{15}$$

4. Results and discussion

Based on the above model and calculation method, the mechanical behavior of drillstring in sliding drilling operation is studied. A horizontal well is drilled of which the depth of kick-off point is 500 m, the inclination angle of the horizontal section is approximately $\pi/2$ and the total well depth is 3000 m. The hole diameter is 0.2159 m. A 5-1/2″drill pipe is adopted of which drill string weight in air per unit length is 28.03 kg/m, Bingham drill fluid is used of which the density is 1.2 g/cm^3. The viscosity of the drilling fluid is 0.2 Pa•s. The drag increase coefficient is 3. The rotation speed is 50 rad/s, the rate of penetration is 15 m/h, and four oscillators are arranged below the kick off point. The excitation frequency of the oscillator is 5 Hz, and the excitation load changes in sine function with respect to time.

In the numerical simulation, to reveal the transition between

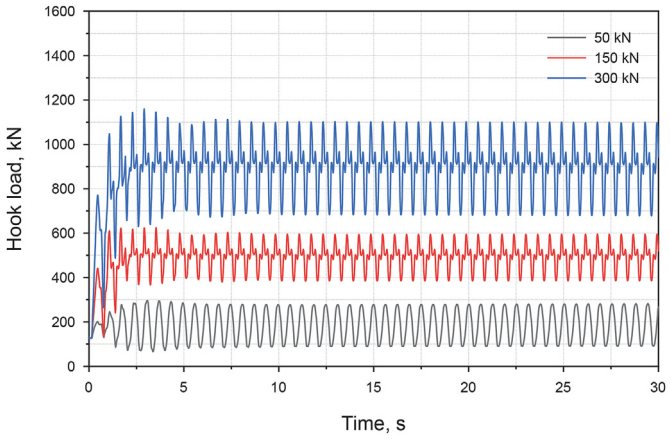

Fig. 18. Effect of vibration amplitude on hook load.

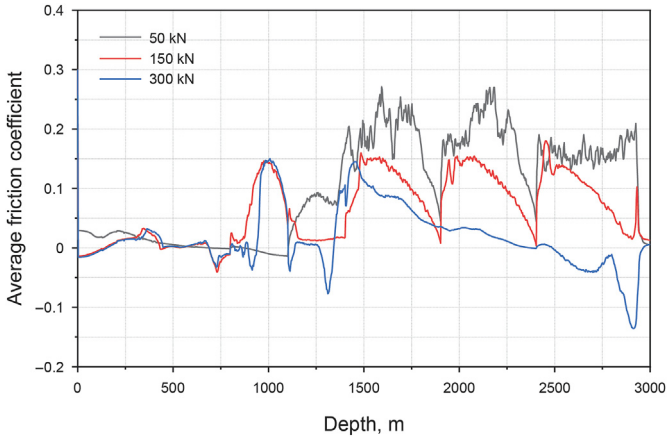

Fig. 19. Effect of vibration amplitude on average friction coefficient.

sticking friction and sliding friction, the time interval should be very small. The time interval is set to 4e-4 s, segment length is set to 3 m, operation time is set to 30 s. It takes about 30 s to obtain the results.

4.1. Vibration behavior

As shown in Fig. 4, during the sliding drilling operation, when the drill bit breaks rock at the set drilling speed, the axial displacement of the drillstring increases. When the drillstring starts to move, the displacement increases more rapidly. As the time increases, the movement of the drillstring enters a stable state, the displacement oscillates around its average value.

As shown in Fig. 5, during the sliding drilling operation, the friction coefficient of the drillstring always shows a regular change. Generally speaking, because the vibration of the drillstring is nonlinear, and the friction coefficient is opposite to the direction of the movement of the drillstring, the change of the friction coefficient is not constant. When the drillstring moves in the positive direction, it always transitions from the static friction coefficient to the dynamic friction coefficient in the form of a parabola, and then returns to the static friction coefficient with the same law, and finally changes the direction of movement and reciprocates with the same law. In other words, the friction coefficient first decreases and then increases, and the direction of change also decreases first and then increases, and then continues to reciprocate.

As shown in Fig. 6, the velocity of the drillstring presents a relatively regular movement pattern, the drillstring is in an unstable state at the beginning of the movement, and the fluctuation of the drillstring velocity is not stable. With an increase in time, the velocity change amplitude gradually stabilizes, and the velocity always reciprocates around the zero point.

As shown in Fig. 7, since the top of the drillstring is always controlled by the hook, the changes of hook load can reflect the working conditions of the bottom hole drillstring and bit in real time. At the beginning of drilling, the hook load is relatively small. With an increase in time, combined with the action of the downhole oscillator, the hook load increases rapidly and reaches a stable state. The load always oscillates around an average value. It can be seen that in the sliding drilling process, the increase in the hook load is more obvious, indicating that the axial friction is decreased a lot and the sliding drilling process is more smooth.

As shown in Fig. 8, due to the excitation of the oscillator, the contact force of the drillstring is particularly unstable in the bending section, the curve change is not smooth. But it can be found that where oscillators are installed are several obvious mutation points, indicating that the oscillator plays a certain role here. But as to whether the performance of power or resistance is not obvious, the following will be verified by comparison.

As shown in Fig. 9, the axial force of the drillstring jumps to varying degrees at the oscillator installation position, resulting in a

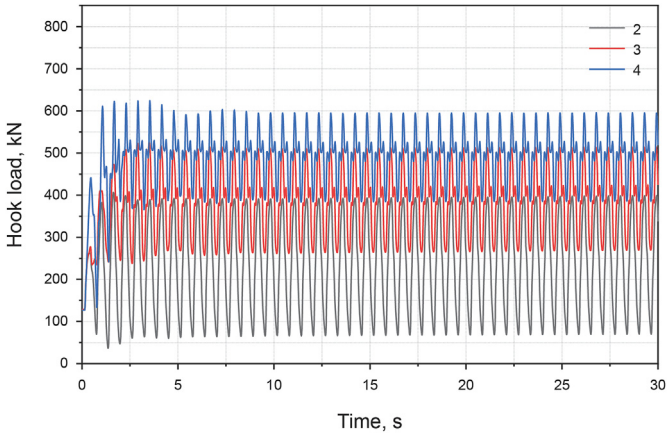

Fig. 20. Effect of the oscillator number on hook load.

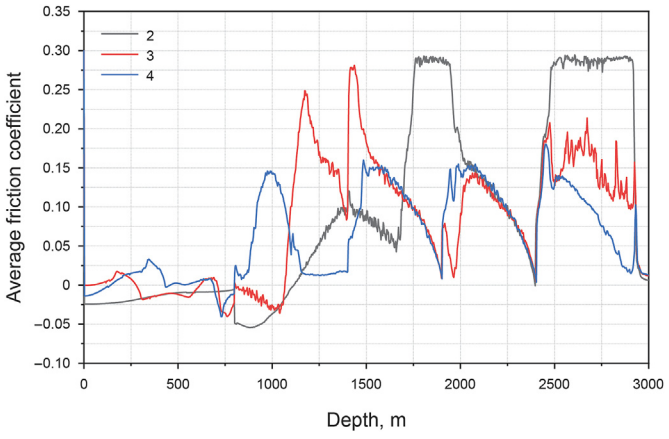

Fig. 21. Effect of the oscillator number on average friction coefficient.

discontinuous axial force. This may be different from the conventional understanding of axial force distribution. But considering the effect of the oscillator at this point, the rationality of the model cannot be verified.

4.2. Drag reduction of oscillator

Before optimizing the parameters, the mechanical behavior of the drillstring with and without oscillator are first analyzed. To simulate the no oscillator case, the excitation force of the oscillator is set to zero in the above model.

The calculation results with and without oscillator are shown in Figs. 10–14. Figs. 10 and 11 show that when the oscillator is installed on the drillstring, the displacement of the drillstring and the hook load increase greatly, showing a more severe fluctuation pattern. But the displacement of the drillstring and the hook load without the oscillator basically have no change, only a slight jump at the beginning of the movement, and then it is stable. This indicates that the drillstring with oscillator is excited by the excitation force, the load transfer is more obvious, and the drillstring has been in motion. Figs. 12 and 13 show that when the oscillator is not installed on the drillstring, the contact force and axial force are continuous, and the curve changes relatively smoothly. The contact force and axial force of the drillstring installed with the oscillator are greatly increased, which is due to that the action of excitation force will break the original equilibrium state of the drillstring. The excitation force applied to the drillstring will change the axial force distribution of the drillstring, thereby changing the contact force of the drillstring. Thus, the oscillator can change the transfer of the axial force of the drillstring substantially. A comparison between the average friction coefficients of the drillstring with and without the oscillator are given in Fig. 14. The average friction coefficient of the drillstring with the oscillator will be greatly reduced, especially at the installation location of the oscillator. The decrease in the average friction coefficient of the drillstring is very obvious. The analysis of the above results shows that the load transfer on drillstring with the oscillator is much better than that without oscillator, and the average friction coefficient is greatly reduced. The field operation shows that the friction of drilling tools can be reduced by 75%–80% when the oscillator is selected with appropriate parameters. The results of the model in this paper show that the friction of drillstring is reduced by 78.4%, which is basically consistent with the field data, thus verifying the rationality of this model.

4.3. Oscillator optimization

Through the above analysis, we have known that the drillstring with the oscillator can play a drag reduction effect in the sliding drilling processes. In this section, relevant parameters including excitation force form, vibration amplitude, oscillator number, etc. are optimized to maximize the effect of drag reduction.

The evaluation of the drag reduction effect under different vibration forms of the excitation force is shown in Figs. 15–17. As shown in Fig. 15, oscillators with different amplitudes and vibration frequencies generate the same impulse in one cycle to ensure that the oscillator can provide the same load in the same cycle. As shown in Fig. 16, the vibration force of larger amplitude has a greater impact on the hook load. The vibration function form has basically no effect on the average hook loads, because the oscillator can generate the same vibration impulse in the same period. As shown in Fig. 17, when the vibration impulse is the same, the vibration function form with larger amplitude and smaller frequency has the most obvious effect on reducing the average friction coefficient. But when the amplitude increases and the frequency decreases to a certain degree, the drag reduction effect stabilizes in a good state.

The evaluation of the vibration amplitude on drag reduction effect is shown in Figs. 18 and 19. As shown in Fig. 18, the larger the vibration force amplitude, the larger the average hook load and the fluctuation amplitude of hook load, indicating that large vibration force amplitude is the key factor improving the axial force transfer along the drillstring; as shown in Fig. 19, the amplitude increases, the average friction coefficient decreases, indicating that the large vibration force amplitude has a significant effect on reducing the average friction coefficient. However, if the amplitude is too large, the drillstring is subjected to alternating loads, which may lead to the risk of slippage of the drill pipes joint and fatigue damage of the drillstring.

The evaluation of the number of oscillators on drag reduction effect is shown in Figs. 20 and 21. As shown in Fig. 20, the more oscillators there are, the more severe the hook loads fluctuation are, and the average hook load increases significantly, indicating that the number of oscillators is crucial to the transmission of axial force of the drillstring. As shown in Fig. 21, the more oscillators, the lower the average friction coefficient of the drillstring, indicating that multiple oscillators can significantly decrease the average friction coefficient. However, too many oscillators may lead to large hydraulic power loss and high risk of drillstring fatigue.

5. Conclusions

According to the above analysis, several conclusions can be drawn as follows.

(1) A dynamic model of drillstring with drag reduction oscillators is established with the bilinear hysteretic restoring model depicting friction force, which provides the basis of mechanical analysis and optimal design of drillstring with drag reduction oscillators.
(2) When downhole oscillators are installed on drillstring in sliding drilling operations, the hook load increases obviously, and the average friction coefficient is decreased significantly. Therefore, downhole oscillators can decrease the axial friction force and increase sliding drilling limits.
(3) With increases in the number of drag reduction oscillators and amplitude of vibration force, the average friction coefficient and the axial friction are both decreased. Meanwhile, the risk of drillstring fatigue and the loss of hydraulic energy are also increased a lot, which is detrimental to safe drilling operation. Therefore, there exist the optimal number of oscillators and amplitude of vibration force.

Acknowledgments

The authors gratefully acknowledge the financial support from the Natural Science Foundation of China (Grant Nos. 51904317, 51821092, U1762214) and Science Foundation of China University of Petroleum, Beijing (Grant No. ZX20180414).

References

AlZibde, A., AlQaradawi, M., Balachandran, B., 2017. Effects of high frequency drive speed modulation on rotor with continuous stator contact. Int. J. Mech. Sci. 131–132, 559–571. https://doi.org/10.1016/j.ijmecsci.2017.08.004.
Baez, F., Barton, S.P., 2011. Delivering performance in shale gas plays: Innovation technology solutions. SPE/IADC Drilling Conference and Exhibition, Amsterdam, Netherlands. https://doi.org/10.2118/140320-MS.
Baker HD, Claypoole W, Fuller DD. Proceedings of the First U.S. National Congress of Applied Mechanics Held at Illinois Institute of Technology, Illinois, Chicago, USA, 11-16 June 1951.
Bavadiya, V.A., Alsaihati, Z., Ahmed, R., et al., 2017. Experimental investigation of the

effects of rotational speed and weight on bit on drillstring vibrations, torque and rate of penetration. SPE Abu Dhabi international Petroleum Exhibition & Conference, Abu Dhabi, UAE. https://doi.org/10.2118/188427-MS.
Denison, E.B., 1979. High data-rate drilling telemetry system. J. Petrol. Technol. 31 (2), 155–163. https://doi.org/10.2118/6775-pa.
Fridman, H.D., Levesque, P., 1959. Reduction of static friction by sonic vibration. J. Appl. Phys. 30 (10), 1572–1575. https://doi.org/10.1063/1.1735002.
Ho, H.S., 1988. An improved modeling program for computing the torque and drag in directional and deep wells. SPE Annual Technical Conference and Exhibition, Houston, TX. https://doi.org/10.2118/18047-MS.
Iwan, W.D., 1961. The Dynamic Response of Bilinear Hysteretic Systems. PhD dissertation. Pasadena. California Institute of Technology.
Johancsik, C.A., Friesen, D.B., Dawson, R., 1984. Torque and drag in directional wells-prediction and measurement. J. Petrol. Technol. 36 (6), 987–992. https://doi.org/10.2118/11380-pa.
Li, B., 2014. Development and pilot test of hydro-oscillator. Petroleum Drilling Techniques 42 (1), 111–113. https://doi.org/10.3969/j.issn.1001-0890.2014.01.022 (in Chinese).
Li, Z.F., Zhang, Y.G., Hou, X.T., et al., 2004. Analysis of longitudinal and torsion vibration of drillstring. Eng. Mech. 21 (6), 203–210 (in Chinese).
Li, Z.F., Yang, H.B., Xu, C.T., et al., 2013. Bit feed principles and technologies in slide-drilling directional wells. Nat. Gas. Ind. 33 (12), 94–98. https://doi.org/10.3787/j.issn.1000-0976.2013.12.014 (in Chinese).
Liao, C.-M., Vlajic, N., Karki, H., et al., 2012. Parametric studies on drill-string motions. Int. J. Mech. Sci. 54, 260–268. https://doi.org/10.1016/j.ijmecsci.2011.11.005.
Lin, Y.Q., Wang, Y.H., 1990. New mechanism in drilling vibration. In: Offshore Technology Conference, Houston, Texas, 7-10 May. https://doi.org/10.4043/6225-MS.
Liu, X.B., Vlajic, N., Long, X.H., et al., 2014. Coupled axial-torsional dynamics in rotary drilling with state-dependent delay: stability and control. Nonlinear Dynam. 78, 1891–1906. https://doi.org/10.1007/s11071-014-1567-y.
Liu, X.B., Long, X.H., Zheng, X., et al., 2020. Spatial-temporal dynamics of a drill string with complex time-delay effects: bit bounce and stick-slip oscillations. Int. J. Mech. Sci. 170. https://doi.org/10.1016/j.ijmecsci.2019.105338.
Miska, S.Z., Zamanipour, Z., Merlo, A., et al., 2015. Dynamic soft string model and its practical application. SPE/IADC Drilling Conference and Exhibition, London, England, UK. https://doi.org/10.2118/173084-MS.
Newman, K., Burnett, T., Pursell, J., et al., 2009. Modeling the affect of a downhole vibrator. SPE/ICoTA Colied Tubing and Well Intervention Conference, Woodlands, Texas, USA. https://doi.org/10.2118/121752-MS.
Pohlman, R., Lehfeldt, E., 1969. Influence of ultrasonic vibration on metallic friction. Ultrasonics 4 (4), 178–185. https://doi.org/10.1016/0041-624X(66)90244-7.
Skyles, L., Amiraslani, Y., Wilhoit, J., 2012. Converting static friction to kinetic friction to drill further and faster in directional holes. SPE Drilling Conference and Exhibition, San Diego, California. https://doi.org/10.2118/151221-MS.
Sola, K.-I., Lund, B., 2000. New downhole tool for coiled tubing extended reach. SPE/ICoTA Colied Tubing Roundtable, Houston, Texas, USA. https://doi.org/10.2118/60701-MS.
Wang, J., Xia, C.Y., Feng, D., et al., 2016. Design and experimental study on a new type of turbine driven hydraulic oscillator. Chinese Journal of Engineering Design 23 (4), 391–395. https://doi.org/10.3785/j.issn.1006-754X.2016.04.015 (in Chinese).
Wang, P., Ni, H.J., Wang, X.Y., et al., 2018. Modelling the load transfer and tool surface for friction reduction drilling by vibration drill-string. J. Petrol. Sci. Eng. 164, 333–343. https://doi.org/10.1016/j.petrol.2018.01.078.
Zhang, H., Yu, W.T., Chen, Z.S., et al., 2014. Development of hydropulse axial-oscillation friction-reduce tool. Oil Field Equipment 43 (7), 73–76. https://doi.org/10.3969/j.issn.1001-3842.2014.07.019 (in Chinese).
Zheng, X., Agarwal, V., Liu, X.B., et al., 2020. Nonlinear instabilities and control of drill-string stick-slip vibrations with consideration of state-dependent delay. J. Sound Vib. 473. https://doi.org/10.1016/j.jsv.2020.115235.